

# Lipidic Membranes Are Potential “Catalysts” in the Ligand Activity of the Multifunctional Pentapeptide Neokyotorphin

Sílvia C. D. N. Lopes,<sup>[a]</sup> Aleksander Fedorov,<sup>[a]</sup> and Miguel A. R. B. Castanho<sup>\*[b]</sup>

*Neokyotorphin (NKT) is a multifunctional pentapeptide that is involved in biological functions as diverse as analgesia, anti-hibernatic regulation and proliferation stimulus of tumour cells. The interaction of neokyotorphin with cell membranes is potentially important to all these multiple biological processes since receptor-mediated processes are thought to be involved in neokyotorphin action. Sargent and Schwyzer proposed in their “membrane catalysis” model that ligands interact with membrane lipids in order to adopt the necessary conformation for cell receptors. We have used fluorescence techniques to study the depth, orientation and extent of incorporation of NKT with model mem-*

*brane systems (lipidic vesicles). The roles of lipid charge, membrane phase and sterol presence were investigated. The phenolic ring of tyrosine is located in a shallow position in membranes. The extent of partition is less in gel crystalline membranes than in liquid crystalline membranes. Addition of cholesterol causes a reorientation of the tyrosine ring at the interface of lipidic bilayers. Lipidic membranes meet all the conditions required for acting as potential “catalysts” in the ligand activity of the multifunctional pentapeptide NKT, because they modulate the exposure and orientation of the phenolic ring, which is most likely involved in docking to receptors.*

## Introduction

Neokyotorphin (NKT) is a multifunctional pentapeptide (H-Thr-Ser-Lys-Tyr-Arg-OH; Figure 1) that was first isolated from bovine brain by Takagi et al.<sup>[1]</sup> NKT is one of the last peptides obtained from haemoglobin  $\alpha$ -chain hydrolysis and contains in its C terminus the sequence of the powerful endogenous analgesic neuropeptide, kyotorphin (L-Tyr-L-Arg; KTP).<sup>[2]</sup> NKT also possesses neuroactivity, but it has been suggested that different analgesic mechanisms are involved in the actions of these two related peptides.<sup>[3]</sup> Moreover, NKT is involved in anti-hibernatic regulation<sup>[4]</sup> and in stimulating the proliferation of L929 tumour cells<sup>[5]</sup> through proposed receptor-mediated processes.<sup>[6,7]</sup> The interaction of NKT with cell membranes is potentially important to all these biological processes. Sargent and

Schwyzer proposed in their “membrane catalysis” model that peptides could interact with membrane lipids in order to adopt the necessary conformation for docking cell receptors.<sup>[8]</sup> This way, the molecular mechanism of receptor-mediated processes is based both on receptor and membrane requirements. The tyrosine residue’s location and orientation in neuropeptides is a crucial factor for both interaction with cell receptors and biological activity, as observed for enkephalin peptides<sup>[9]</sup> for instance. NKT’s phenolic ring exposure and orientation are therefore very likely to be key requirements for NKT interaction with receptors and for its biological activity. Moreover, NKT possesses in its structure two amino acid residues, lysine and arginine, that are adjacent to the tyrosine residue and are known to act as peptide anchors in membranes.<sup>[10]</sup> It is our goal to report structural information on NKT interactions with model systems of biological membranes. We have used the intrinsic fluorescence of tyrosine to study the location, orientation and extent of NKT insertion in model membranes systems. The influence of membrane charge, lipid phase and sterol presence were investigated.

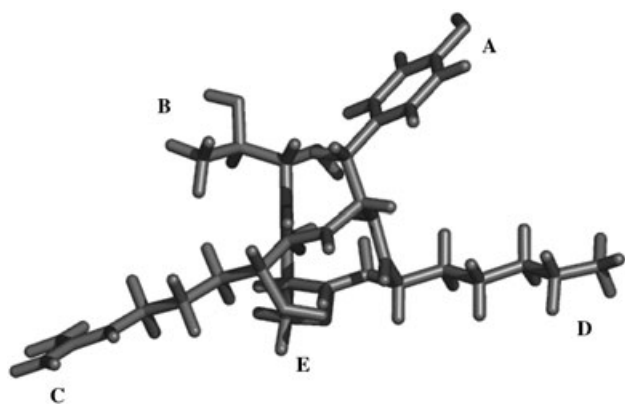


**Figure 1.** NKT structure: A) tyrosine side chain (phenolic ring), B) threonine side chain (positively charged N terminus), C) arginine side chain positively charged (C terminus), D) lysine side chain (positively charged) and E) serine side chain.

[a] S. C. D. N. Lopes, Dr. A. Fedorov  
Centro de Química-Física Molecular, Instituto Superior Técnico  
Av. Rovisco Pais, 1049-001 Lisboa (Portugal)

[b] Prof. M. A. R. B. Castanho  
Centro de Química e Bioquímica  
Faculdade de Ciências da Universidade de Lisboa  
Campo Grande, Ed. C8, 1749-016 Lisboa (Portugal)  
Fax (+35) 121-750-0088  
E-mail: castanho@fc.ul.pt

## Results and Discussion

NKT absorption and emission spectra in different media are represented in Figure 2. Except for NKT absorption spectra in multibilayer systems, all spectra have vibronic progression and

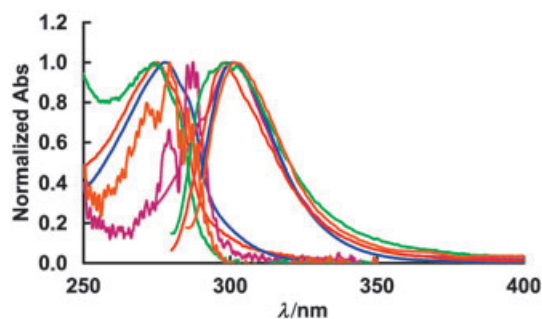


**Figure 2.** NKT absorption and emission spectra in acetate buffer (20 mM, pH 4.94, red), ethanol (blue), POPG (3 mM) LUVs (green), POPG multibilayers (pink) and POPG plus cholesterol multibilayers (orange). Only POPG-containing systems are represented for the sake of clarity; similar spectra were obtained for DPPC systems.

energy ranges that are characteristic of L-tyrosine. A slight absorption/emission red shift is observed when NKT is in lipidic systems (Figure 2 and Table 1) or in ethanol; this points to the

**Table 1.** Photophysical parameters for NKT in acetate buffer (20 mM, pH 4.94), ethanol, POPC LUVs (pH 4.94) and POPC multibilayers (pH 4.94); maximum absorption and emission wavelength ( $\lambda_{\text{Abs}}$ ,  $\lambda_{\text{Em}}$ ), fluorescence quantum yield ( $\Phi_F$ ) and mean lifetime ( $\bar{\tau}$ ).

|                | $\lambda_{\text{Abs,max}}$ [nm] | $\lambda_{\text{Em,max}}$ [nm] | $\Phi_F$ | $\bar{\tau}$ [ns] |
|----------------|---------------------------------|--------------------------------|----------|-------------------|
| acetate buffer | 275                             | 298                            | 0.03     | 1.15              |
| EtOH           | 278                             | 301                            | –        | –                 |
| LUVs (5 mM)    | 274                             | 303                            | 0.06     | 3.27              |
| Multibilayers  | 278 and 286                     | 303                            | –        | –                 |

fact that the tyrosine in NKT is slightly sensitive to the polarity of the environment. This is a peculiarity since tyrosine emission, at variance with tryptophan, is generally rather insensitive to the local environment. A complex combination of 1) the ability of phenolic rings to engage excitonic coupling, as demonstrated in the phenolic-related chromophores of Triton X-100,<sup>[11]</sup> together with 2) concomitant multiple solvent effects<sup>[12,13]</sup> prevents a detailed explanation for the altered vibronic progression with a simultaneous small red shift. Phenol absorption in heptane shows moderately sharp vibrational resolution, at variance with spectra in ethanol.<sup>[12]</sup> When the

substituents of benzene are polar groups, the fine structure disappears in polar solvents. The effect of auxochromes (such as OH) on the fine structure of the 260 nm bands of benzene is explained in terms of the interaction of the unshared electrons with the benzene nucleus.<sup>[12]</sup> Peptide clustering and/or the concealment of the phenolic rings in the membrane result in the albeit weak vibrational resolution observed in lipidic multibilayers, compared to its absence in homogeneous solution and lipidic vesicles.

Fluorescence quantum yield ( $\Phi_F$ ) and mean lifetime ( $\bar{\tau}$ ) of NKT both in homogeneous aqueous solution and in the presence of large unilamellar vesicles (LUVs) are presented in Table 1. Higher values are obtained when the peptide is in the presence of lipidic bilayers; this further demonstrates that the phenolic ring is interacting with the lipidic vesicles. However both values are lower than the ones obtained for free L-tyrosine in buffer solution.<sup>[14]</sup> Several authors<sup>[15,16]</sup> have suggested that the fluorescence of an aromatic amino acid side chain can be quenched by the peptide group as a consequence of a charge transfer between the excited chromophore (phenol ring), acting as a donor, and electrophilic units in the amino acid backbone, acting as acceptors. Moreover, Ross et al.<sup>[17]</sup> also observed that, if the phenol side chain is shielded from solvent and the local environment contains no proton acceptors, many intra- and intermolecular interactions result in a reduction of the quantum yield.

NKT prefers liquid crystalline to gel crystalline phase systems; the partition coefficient,  $K_p$ , in 1-palmitoyl-2-oleoyl-*sn*-glycero-3-phosphatidylcholine (POPC) is higher than the  $K_p$  in L- $\alpha$ -dipalmitoylphosphatidylcholine (DPPC) vesicles, (Table 2). Cholesterol addition to liquid-crystalline-phase systems decreases the partition coefficient (Table 2), which is expected given its condensation effect. Apparently increased negative surface charge has no significant effect on the binding of NKT (Table 2). The present study was carried out at pH 4.94 to ensure that the peptide is positively charged. Electrostatic attraction is known to play an important role in the binding of many positively charged peptides and proteins to negatively charged bilayers.<sup>[18]</sup> At pH 4.94 and a salt concentration of 20 mM most of the 1-palmitoyl-2-oleoyl-*sn*-phosphatidylglycerol (POPG) is fully deprotonated<sup>[19,20,21]</sup> with a  $-1$  net charge in its polar head group. However, it seems to have no effect, whatsoever on NKT interaction with lipids. In fact, similar  $K_p$ 's

**Table 2.** Partition coefficient constant ( $K_p$ ), Stern–Volmer quenching constant ( $K_{SV}$ ), second rank order parameter ( $\langle P_2 \rangle$ ), mean angle ( $\langle \Psi \rangle$ ) displacement from the bilayer normal, fraction of the fluorescence intensity emitted by the peptide incorporated in the membrane ( $f_I$ ) and fraction of the peptide which is accessible to the quencher ( $f_B$ ) in different lipid systems at pH 4.94.

| System | Cholesterol | $K_p \times 10^{-3}$ | $K_{SV} \times 10^{-3} [\text{M}^{-1}]$ | $\langle P_2 \rangle$ | $\langle \Psi \rangle$ | $f_I$ | $f_B$ |
|--------|-------------|----------------------|---|-----------------------|------------------------|-------|-------|
| POPC   | –           | $1.98 \pm 0.6$       | 0.057                                   | 0.641                 | 29.29                  | 0.94  | 0.94  |
| DPPC   | –           | $0.12 \pm 0.05$      | –                                       | –                     | –                      | –     | –     |
| POPG   | –           | $2.1 \pm 0.4$        | 0.031                                   | 0.662                 | 28.34                  | 0.96  | 0.90  |
|        | +           | $0.31 \pm 0.02$      | $5.7 \pm 0.8$                           | 0.472                 | 36.39                  | 0.78  | 0.48  |

– and +, in the cholesterol column denote the absence or presence of cholesterol (33% molar) in the system studied, respectively. KI or cholesteryl bromide were used as quenchers in systems without and with cholesterol, respectively (lipid concentration = 5 mM, cholesterol<sub>total</sub> concentration = 1.65 mM).

were obtained for the peptide in presence of negatively charged membranes (POPG) compared with zwitterionic membranes (POPC). NKT possesses in its structure two charged amino-acid residues, lysine and arginine, adjacent to the tyrosine residue that have flexible apolar long side chains with charged terminal groups. Interfacial partitioning of lysine and arginine has been assumed to be relatively favourable due to the hydrophobic interaction of their methylenes with the membrane interface, whereas their charged groups would have unfavourable contributions and interact with the aqueous phase ("snorkel effect"<sup>[10]</sup>). Although White and Wimley were unable to observe this effect in their pentapeptides,<sup>[10]</sup> interfacial partitioning might become predominantly favourable if peptides have aromatic residues, as is the case for tyrosine (Figure 3). Threonine and serine make small contributions.<sup>[10]</sup>

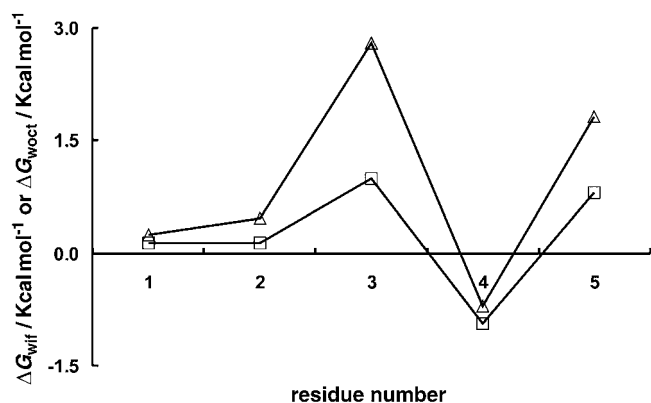


**Figure 3.** Theoretical analysis of partition of NKT into lipidic membranes. □ and △ denote  $\Delta G_{wif}$  and  $\Delta G_{woct}$ , respectively.  $\Delta G_{wif}$  is the whole-residue free energy balance from water to bilayer interface and  $\Delta G_{woct}$  is the whole-residue free energy from water to octanol. Octanol is commonly used for measurement of bulk-phase hydrophobicities.<sup>[10]</sup>  $\Delta G_{wif} < 0$  denotes a preference of the residue for the membrane interface and  $\Delta G_{wif} > 0$  a preference of the residue for the aqueous environment.

To explain the apparent lack of effect of electrostatic interactions on peptide partitioning in membranes, we propose that the "additional" uptake of peptides by the lipidic bilayers, which is due to charge effects, occurs at a very superficial level; this leaves the chromophoric phenolic ring totally exposed to the aqueous medium (Figure 4). This subpopulation of fully exposed chromophores does not make a large contribution to  $K_p$  calculation because it does not experience an increase in quantum yield due to binding (i.e., the fluorescence quantum yield is similar to unbound NKT). In zwitterionic lipids, lysine and arginine bury themselves with their aliphatic chains inside the lipid bilayer, while positioning the charged group in the aqueous interface of the bilayers (Figure 4A). This allowed the phenolic group to penetrate deeper in the lipid head groups, and therefore resulted in increased fluorescence quantum yield. In negatively charged bilayers, the positively charged lateral chains of lysine and arginine become more restricted in their depth location in the bilayer; this forces the phenolic ring of tyrosine to a shallower location (Figure 4B). The phenolic ring is projected from the plane that includes the

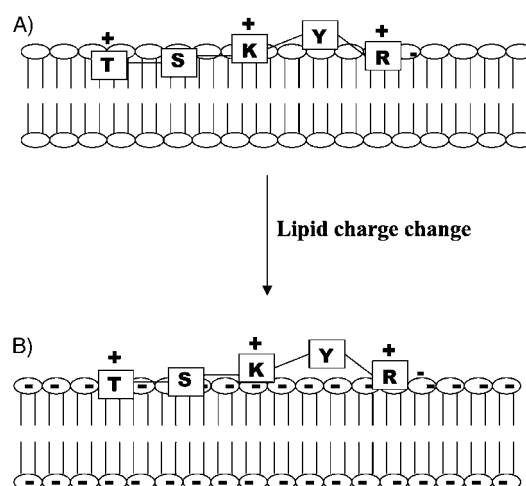


**Figure 4.** Schematic view of NKT depth location in A) zwitterionic lipids where the lysine (K) and arginine (R) side chains are able to bury their aliphatic part inside the lipid bilayer, while positioning the charged group in the aqueous interface of the bilayers. The phenolic group is thus allowed to penetrate deeper into the lipids' head group and therefore, has an increased fluorescence quantum yield. B) In negatively charged lipids, where the positively charged lateral chains of lysine and arginine become more restricted in their depth location in the bilayer, the phenolic ring of tyrosine (Y) is forced to a shallower location. T and S are threonine and serine amino-acid residues. + and - denote the formal charge in each amino acid at pH 4.94.

positively charged groups of the molecule. (One can speculate this would be the negatively charged bilayer plane, Figure 4B.)

Fluorescence-quenching studies were performed to confirm the location of NKT's phenolic ring in the different systems. Cholesteryl bromide and iodide anions ( $I^-$ ) were used as quenchers of NKT fluorescence in the presence of bilayers with or without cholesterol, respectively. The ability or not of the quenchers to decrease tyrosine fluorescence can be used to determine the degree of exposure of this amino acid residue to the aqueous phase or lipidic interface.  $I^-$  is able to quench tyrosine residues that are exposed to the aqueous phase. The bromide quencher in cholesteryl bromide replaces the -OH group in cholesterol and is putatively at the same depth in the lipidic bilayers interface. It is thus able to quench phenolic rings at this depth. If the fluorophore is exposed to the aqueous medium, a considerable fraction of the emitted fluorescence will be quenched by  $I^-$ . On the other hand if it is buried in the lipidic head group interface (i.e., in the quencher vicinity) quenching by cholesteryl bromide will be effective. The fraction of fluorescence intensity accessible to each quencher ( $f_b$ ) was determined by application of the Lerher equation<sup>[22]</sup> to the data (Figure 5), whereas the fraction of fluorescence intensity emitted from the lipidic environment ( $f_l$ ) was determined from  $K_p$  as described in ref. [23]. According to the results presented in Table 2, we can conclude that at lipidic concentrations of  $[POPG] = [POPC] = 1$  mM, almost all of the fluorescence signal originated from peptides that interacted with lipidic membranes ( $f_l \approx 1$ ), and  $f_b$  is close to 1. This means that the fraction of phenolic rings buried in the membrane is very small. When cholesterol is added to POPG, its condensation effect has a severe influence in hindering the insertion of the

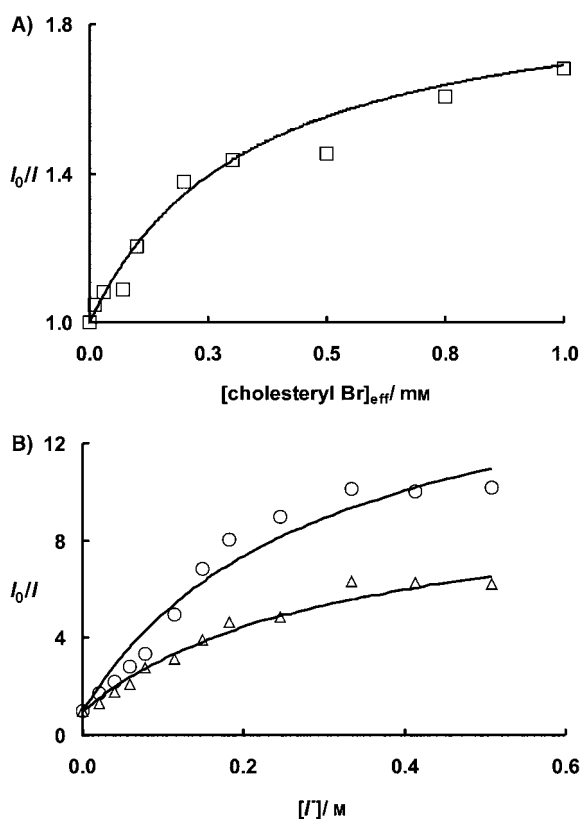


**Figure 5.** Stern–Volmer plot for the fluorescence quenching of NKT by A) cholesteryl bromide in POPG plus cholesterol ( $\square$ ) LUVs (33% molar of total sterol–cholesterol plus cholesteryl bromide) and by B)  $I^-$  in the presence of POPC ( $\circ$ ) and POPG ( $\triangle$ ) vesicles.

phenolic ring in lipidic palisades (therefore  $K_p$  and  $f_L$  decrease). With cholesteryl bromide as fluorescence quencher,  $f_B/f_L = 60\%$ ; this means that only 60% of the tyrosine residues in the lipidic membranes are buried deep in the lipidic head-group interface. The remaining 40% are very shallow in the membrane. Therefore, we conclude that there is a high degree of exposure of the tyrosine ring to the aqueous-phase bulk environment, both in cholesterol-free and cholesterol-rich lipidic membranes.

Cholesterol plays a role in NKT orientation. The lowest-energy singlet transition of tyrosine is due to the  $^1L_b$  transition, oriented across the phenyl ring (Figure 6), with an absorption maximum of approximately 277 nm.<sup>[17]</sup> For an excitation wavelength above 260 nm, the electronic absorption and emission occurs from the same  $^1L_b$  state, and orientation of the phenolic ring can be obtained.<sup>[24]</sup> The phenolic ring orientation is influenced by the presence of cholesterol (Table 2). The second rank order parameter suggests that the transition moment is at an intermediate position between perpendicular and parallel to the lipidic membrane surface. Although not dramatic, cholesterol seems to increase on average the angle between the bilayer normal (system director axis) and the phenolic transition moment. It is not possible to conclude from the data if this displacement is in-plane (Figure 6A), out-of-plane (Figure 6B) or both.

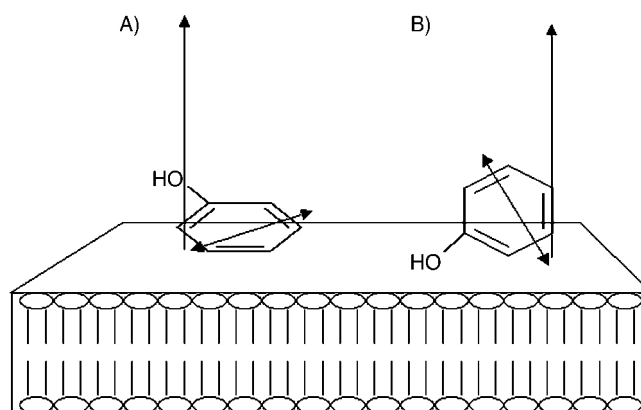


**Figure 6.** Angular displacements relative to the director axis (ZZ) might occur A) out-of-plane or B) in-plane.  $^1L_b$  allowed transition in the phenolic ring is denoted with the horizontal double arrow.

## Conclusion

In spite of its hydrophilic character, the multifunctional pentapeptide NKT interacts with the models of biological membranes. The observed interaction with membranes' surfaces putatively meets the orientational constraints needed for receptor–ligand interaction. Altered peptide diffusion and protection from proteolytic processes might be additional outcomes. A shallow location of the phenolic ring of tyrosine was concluded, mainly in charged membranes. Phenolic groups are common in biologically active peptides and are involved in the interaction with cell receptors (e.g., enkephalins, endorphins and related molecules<sup>[9]</sup>). Exposure and orientation are crucial for molecular recognition through cellular receptor-mediated processes, such as the ones proposed for NKT.<sup>[4,5]</sup> This study demonstrates that the phenolic ring of NKT is exposed to receptor interaction with a well-defined orientation relative to the bilayer plane. Therefore, the structural requirements needed for the biological membranes to act as “catalysts” are met. The “membrane catalyst” hypothesis, which states that the membrane's role is to allow ligands to adopt the necessary docking constraints for cell receptors,<sup>[6]</sup> is of general acceptance and is based mainly on chemical intuition. However, extensive experimental support for this hypothesis is still lacking. This paper presents evidence that critical ligand groups might indeed be exposed and oriented by lipidic membranes, in order to adopt cellular receptor requirements.

## Experimental Section

NKT (Bachem, Switzerland), cholesterol, cholesteryl bromide and 5-methoxyindole (Sigma, St. Louis, Mo, USA) were 99% pure. All lipids were from Avanti Polar Lipids (Alabaster, AL, USA). The solvents were from Merck (Darmstadt, Germany) and of spectroscopic grade.

UV/Vis absorption measurements were carried out in a Shimadzu spectrophotometer (model UV-3101 PC).

A spectrofluorimeter SLM-Aminco 8100 equipped with a 450 W Xe Lamp and double monochromators for both excitation and emis-

sion, as well as a quantum counter was used. Excitation and emission wavelengths were 277 nm and 303 nm, respectively.

**Fluorescence decays:** Fluorescence-decay measurements were carried out with a time-correlated single-photon counting system. A frequency doubled, cavity-pumped Rhodamine (Rho) dye laser, synchronously pumped by a mode-locked Ar<sup>+</sup> laser (514.5 nm, Coherent Innova 400–10) was used to excite NKT samples at 285 nm. The emission wavelength was 308 nm. A Hamamatsu R-2809 MCP photomultiplier was used for detection. A Corion W-305-S filter was used to prevent excitation light scattering from interfering with the detected signal.

LUVs were obtained by extrusion<sup>[25]</sup> with NKT and lipid concentrations of  $7 \times 10^{-5}$  M and 5 mM, respectively. Data treatment was as described in ref. [26]. Fluorescence decays were complex and are described by a sum of three exponentials. The mean lifetime, was obtained from:<sup>[14]</sup>

$$\bar{\tau} = \frac{\sum a_i \tau_i^2}{\sum a_i \tau_i} \quad (1)$$

**Partition studies:** Partition studies were carried out in LUVs by using different lipid or lipid plus cholesterol concentrations (up to 5 mM), with a peptide concentration of  $7 \times 10^{-5}$  M. Fluorescence intensity was measured at  $\lambda_{\text{exc}} = 277$  nm and  $\lambda_{\text{em}} = 303$  nm. The measured fluorescence intensity,  $I_f$ , is a balance between the fluorescence intensity of the peptide in bulk aqueous phase ( $I_w$ ) and peptide inserted in the lipidic matrix ( $I_L$ ) [Eq (2)].<sup>[23]</sup> The weight factors in this balance depend on the partition coefficient,  $K_p$ , which was calculated as a fit parameter in a nonlinear-regression methodology and is dimensionless (Figure 7).  $\gamma_L$  denotes the molar volume of the lipid used, and has the reciprocal unities used for the lipid concentration.

$$\frac{I_f}{I_w} = \frac{1 + K_p \gamma_L [L] (I_L/I_w)}{1 + K_p \gamma_L [L]}; K_p = \frac{[NKT]_L}{[NKT]_W} \quad (2)$$

(Here [L] is the lipid concentration; subscripts L and W in [NKT] refer to the lipidic and bulk aqueous media, respectively).

The fraction of the fluorescence intensity emitted by the peptide incorporated in the membrane ( $f_L$ ) can be calculated from:<sup>[23]</sup>

$$f_L = \frac{(I_L/I_w) K_p \gamma_L [L]}{1 + (I_L/I_w) K_p \gamma_L [L]} \quad (3)$$

Details regarding this methodology can be found elsewhere.<sup>[23]</sup>

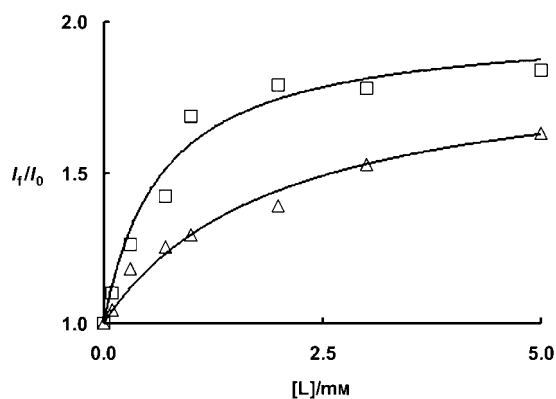


**Figure 7.** Partition curve of NKT in POPC (□) and DPPC (Δ). Solid lines represent the fitting of Equation (2) to the data.

**Quenching studies:** Quenching studies were performed in order to study the depth of NKT's phenolic ring in LUVs with or without cholesterol. In systems without cholesterol, quenching studies were performed by adding small aliquots of KI (0.1 M) to the suspension of LUVs with previously added NKT. In systems containing cholesterol, NKT fluorescence (peptide final concentration  $7 \times 10^{-5}$  M) was quenched by cholesteryl bromide in LUVs (prepared by extrusion as in ref. [25]) of lipid plus cholesterol with increasing concentrations of cholesteryl bromide. The bromide (quencher) replaces the –OH group in cholesterol and is putatively at the same depth in the lipidic bilayer's interface. Briefly, in both cases, the methodology to ascertain the location of the phenolic ring is based on the dependence of the apparent quenching efficiency on the local concentration of the quencher in the vicinity of the fluorophore. If quenching with I<sup>−</sup> and/or cholesteryl bromide occurs, the location of the fluorophore exposed to the bulk phase and/or inserted in the interface (i.e., in the quencher vicinity) can be inferred. Data treatment was as described in ref. [27]. All values of quencher concentration shown in the figures refer to its effective concentration (calculated by means of Equation A1.6 in ref. [28]). Fluorescence intensity was measured with excitation and emission wavelengths of 277 nm and 303 nm, respectively.

The simplest model that describes dynamic or static fluorescence quenching leads to linear Stern–Volmer plots:

$$\frac{I_0}{I} = 1 + K_{SV}[Q] \quad (4)$$

Here  $I_0$  and  $I$  denote the fluorescence intensities in the absence and presence of quencher, respectively,  $K_{SV}$  is the Stern–Volmer constant and  $[Q]$  is the quencher concentration.

However, nonlinear Stern–Volmer plots can also be observed when there are multiple classes of fluorophores in solution.<sup>[28]</sup> Considering that there is a fluorophore population protected from contact with the quencher (A) and a population that is accessible to it (B), quenching data can be analyzed by means of a direct fit of the Lehrer equation:<sup>[19]</sup>

$$\frac{I_0}{I} = \frac{1 + K_{SV}[Q]}{(1 + K_{SV}[Q]_{\text{eff}}) \times (1 - f_B) + f_B} \quad (5)$$

where

$$f_B = \frac{I_0^B}{I_0} \quad (6)$$

$[Q]_{\text{eff}}$  is the effective quencher concentration in the membrane, and  $I_0^B$  is the fluorescence intensity of the fluorophores B in the absence of the quencher.  $K_{SV}$  has units of reciprocal concentration.

A more detailed description of the interpretation of quenching results can be found in ref. [27].

**UV/Vis linear dichroism studies:** Samples of aligned lipid multibilayers, with or without cholesterol, were obtained by semidehydration of liposomes, as described in ref. [24]. The final molar ratios of lipid to NKT and lipid/cholesterol/NKT were 2.5:1 and 1.5:1:1.

UV/Vis absorption and fluorescence measurements were carried out as described in ref. [21]. Namely, second rank order parameters,  $\langle P_2 \rangle$ , were obtained from electronic absorption in aligned multi-

bilayers.  $\langle P_2 \rangle$  is obtained through the dichroic ratio calculated from Equation (7):

$$\frac{\sin(\psi)A_\psi}{A_{\pi/2}} = 1 + \frac{3 \langle P_2 \rangle}{(1 - \langle P_2 \rangle)n^2} \cos^2(\psi) \quad (7)$$

Details regarding this methodology can be found elsewhere.<sup>[24]</sup>

## Acknowledgements

The authors acknowledge Fundação para a Ciência e Tecnologia (Portugal) for funding and grant SFRH/BD/6497/2001 to S.L.

**Keywords:** analgesics • fluorescence • membranes • neokytorphin • vesicles

- [1] H. Takagi, H. Shiomi, K. Fukui, K. Hayashi, Y. Kiso, K. Kitagawa, *Life Sci.* **1982**, *31*, 1733–1736.
- [2] Y. Kiso, K. Kitagawa, N. Kawai, T. Akita, H. Takagi, H. Amano, K. Fukui, *FEBS Lett.* **1983**, *155*, 281–284.
- [3] H. Ueda, M. Ge, M. Satoh, H. Takagi, *Peptides* **1987**, *8*, 905–909.
- [4] I. Y. Popova, Y. M. Kokoz, K. I. Zenchenko, O. S. Vinogradova, *Comp. Biochem. Physiol. Part A, Mol. Integr. Physiol.* **2003**, *135*, 383–402.
- [5] E. Y. Blishchenko, O. A. Mernenko, O. N. Yatskin, R. H. Ziganshin, M. M. Philippova, A. A. Karelin, V. T. Ivanov, *FEBS Lett.* **1997**, *414*, 125–128.
- [6] G. Bronnikov, L. Dolgacheva, S.-J. Zhang, E. Galitovskaya, L. Kramarova, V. Zinchenko, *FEBS Lett.* **1997**, *407*, 73–77.
- [7] M. Salzert, *Placebo* **2002**, *3*, 12–24.
- [8] D. F. Sargent, R. Schwyzer, *Proc. Natl. Acad. Sci. USA* **1986**, *83*, 5774–5778.
- [9] G. L. Patrick, *An Introduction to Medicinal Chemistry*, New York, Oxford University Press, **2001**, 511–550.
- [10] W. C. Wimley, S. H. White, *Nat. Struct. Biol.* **1996**, *3*, 842–848.
- [11] K. Kalyanasundaram, J. K. Thomas in *Micellization, Solubilization & Microemulsions, Vol. 2*, (Ed.: K. L. Mital), Plenum, New York, **1977**, pp. 559–589.
- [12] C. N. R. Rao, *Ultra-violet and Visible Spectroscopy. Chemical Applications*, Butterworth, London, **1967**, pp. 58–75.
- [13] M. Koldřicek, *FEBS Lett.* **1979**, *98*, 295–298.
- [14] J. R. Lakowicz, *Principles of Fluorescence Spectroscopy*, Kluwer/Plenum, New York, **1999**.
- [15] J. E. Tournon, E. Kuntz, M. A. El Bayoumi, *Photochem. Photobiol.* **1972**, *16*, 425–433.
- [16] K. Guzow, R. Ganzynkiewicz, A. Rzeska, J. Mrozek, M. Szablinski, J. Karolczak, A. Liwo, W. Wiczak, *J. Phys. Chem. B* **2004**, *108*, 3879–3889.
- [17] J. B. A. Ross, W. R. Laws, K. W. Rouslang, H. R. Wyssbrod in *Tyrosine Fluorescence and Phosphorescence from Proteins and Polypeptides, Vol 3* (Eds.: J. R. Lakowicz), Plenum, New York, **1992**, pp. 1–63.
- [18] M. Romanowski, X. Zhu, K. Kim, V. J. Hruby, D. F. O'Brien, *Biochim. Biophys. Acta* **2002**, *1558*, 45–53.
- [19] A. Watts, K. Harlos, W. Maschke, D. Marsh, *Biochim. Biophys. Acta* **1978**, *510*, 63–74.
- [20] P. W. M. van Dijck, B. de Kruihff, A. J. Verkleij, L. L. M. van Deenen, J. De Gier, *Biochim. Biophys. Acta* **1978**, *512*, 84–96.
- [21] H. Träuble, M. Teubner, P. Woolley, H. Eibl, *Biophys. Chem.* **1976**, *4*, 319–342.
- [22] S. S. Leher, *Biochemistry* **1971**, *10*, 3254–3263.
- [23] N. C. Santos, M. Prieto, Castanho, *Biochim. Biophys. Acta* **2003**, *1612*, 123–135.
- [24] M. A. R. B. Castanho, S. Lopes, M. Fernandes, *Spectrosc. Int. J.* **2003**, *17*, 377–398.
- [25] M. J. Hope, M. B. Bally, G. Webb, P. R. Cullis, *Biochim. Biophys. Acta* **1985**, *812*, 55–65.
- [26] L. M. S. Loura, A. Fedorov, M. Prieto, *Biochim. Biophys. Acta* **2000**, *1467*, 101–112.
- [27] M. A. R. B. Castanho, M. J. E. Prieto, *Biochim. Biophys. Acta* **1998**, *1373*, 1–16.
- [28] M. Castanho, M. Prieto, *Biophys. J.* **1995**, *69*, 155–168.

Received: September 8, 2004